Temporal–spatial data fusion of structure-borne sound and process signals with optical and radiographic inspection for friction stir welding

Quy R. Luong, Matthias Merzkirch, Markus G. R. Sause

Angaben zur Veröffentlichung / Publication details:

Luong, Quy R., Matthias Merzkirch, and Markus G. R. Sause. 2025. "Temporal–spatial data fusion of structure-borne sound and process signals with optical and radiographic inspection for friction stir welding." Research and Review Journal of Nondestructive Testing (ReJNDT) 2025 (11): 1–10. https://doi.org/10.58286/31935.

Research and Review Journal of Nondestructive Testing (ReJNDT) - ISSN 2941-4989 - www.ndt.net
Selected Papers from the DGZfP Annual Conference 2025

Temporal–Spatial Data Fusion of Structure-borne Sound and Process Signals with Optical and Radiographic Inspection for Friction Stir Welding

Quy R. LUONG[1], Matthias MERZKIRCH[2], Markus G.R. SAUSE[3]

[1] Condition Monitoring, Mechanical Engineering, University of Augsburg, Germany, +49-821-598-69187, quy.raven.luong@uni-a.de
[2] Condition Monitoring, Mechanical Engineering, University of Augsburg, Germany, matthias.merzkirch@uni-a.de
[3] Condition Monitoring, Mechanical Engineering, University of Augsburg, Germany, markus.sause@uni-a.de

Abstract
Data annotation is a mandatory step that enables machine learning methods based on supervised learning. This work introduces a pipeline that aims to reduce the annotation effort by applying data fusion of multiple data modalities e.g. machine data, process acoustics and inspection results related to robotic friction stir welding (FSW). This data is prepared for training machine learning models for assessing the weld quality based on the process acoustics acquired by acoustic emission sensors online in real-time. Non-Destructive Testing (NDT) based on light microscopy and computed tomography (CT) gather weld quality information which are used to annotate the structure-borne sound signals. This work demonstrates how the involved data modalities are put into a shared context by temporal synchronization and definition of common coordinate bases to enable transferring annotations across domains, effectively reducing the amount of annotation effort by a human inspector.

Keywords: acoustic emission, optical inspection, data labelling, data fusion, machine learning

1. Introduction

1.1 Relevance of data annotation in NDT and AI

Artificial intelligence (AI) holds tremendous potential in the field of materials science [1] and fully leveraging this potential requires knowledge in both AI and domain specific knowledge such as Non-Destructive Testing (NDT). However, as these disciplines have traditionally evolved independently from each other, effective interdisciplinary collaboration becomes not only essential but also a significant challenge [2]. Data annotation can be seen as a critical interface between these domains, which enables transferring NDT domain knowledge into data structures usable by AI specialists [3]. It is the process of attaching human-validated information to data aiming to make it usable for downstream tasks e.g. evaluation, decision-making or integration into an automated processing pipeline [4]. Especially for machine learning based approaches, data annotation and its quality are essential as it has for instance a tremendous impact on model performance of welding defect detection [5]. In the context of NDT, this involves characterising defects by type, size, locations or severity and acts as basis for defect classification, quality assurance and compliance with industrial standards. In the context of AI, it enables the generation of data sets with associated results which supervised learning models can learn patterns from to make predictions on new data. However, this annotation process is considered quite expensive [6], primarily because it requires domain knowledge specific to the origin and content of data (i.e. process understanding). The effort is further increased when annotations are created manually (scaling with the amount of data). In the worst-case scenario, annotations are entirely unavailable due to missing expert knowledge or prohibitive efforts, where any supervised learning becomes completely unviable.

To lower the annotation effort, this work will demonstrate a pipeline, which contextually interlocks various data modalities to enable transferring annotations across various domains within a case study that involves the development of a process monitoring system for friction stir welding. This includes data modalities such as structure-borne sound collected by acoustic emission sensors, results from NDT based on light microscopy and computed tomography (CT) to annotate the process acoustics and lastly machine data logging the welding process. Overall,

 https://doi.org/10.58286/31935

this will enable the training of machine learning models for future studies by providing correctly annotated process acoustic data that are otherwise difficult to annotate. Ultimately, this highlights the advantages and importance of digital integration of NDT into production systems like the process monitoring system for friction stir welding, where the welding defects are to be detected and classified online in real-time based on the process acoustics by a machine learning classifier.

1.2 Production process quality inspection

Friction Stir Welding (FSW) is a solid-state joining technique, developed at TWI Ltd in 1991 [7], where a rotating, non-consumable tool is used for continuous connection of the interface of multiple workpieces. This introduces frictional heat, softening the material while staying below the melting point. As the tool asserts high axial force on the materials and moves along their interface, it stirs the malleable materials of the workpieces into each other, resulting in a weld with mechanical properties almost matching the base materials properties [8,9]. Typically, FSW consist of four steps: plunging, dwelling, welding, retraction. During the plunging phase, the rotating tool is introduced into the workpiece until the shoulder makes full contact with the workpiece. Optionally the tool then dwells, remaining in place to allow more heat up. During welding, the tool is often tilted and moves along the desired joint line, leaving behind the welding joint by plastic deformations. To conclude the process, the tool is then retracted, leaving an end crate. The tool consists of a pin and a shoulder. In classical FSW, both rotate, whereas in stationary shoulder FSW only the pin rotates as illustrated in figure 1.

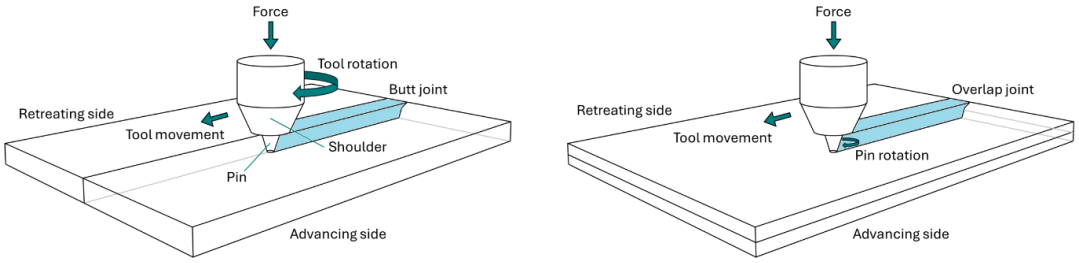

Figure 1. Left: Classical FSW for e.g. butt joints; right: Stationary shoulder FSW for e.g. overlap joints

The primary online process parameters are force, feed, tool orientation and tool rotation speed. Parameters such as material properties of the workpieces [10], the clamping mechanism and the tool design [11] also strongly affect the welding result and are hence typical research and optimization objects as well. After welding, inspection and evaluation are required in accordance with standard such as DIN-ISO 25239-5 [12] providing guidelines for quality assurance and weld inspection. Various surface defects such as surface grooves, irregularities, workpiece offsets, excessive indentation or surface void can be covered by visual inspection. Radiography can be used to inspect e.g. internal voids and deformation, lack of penetration, entrapment of other materials, etc. These defects are to be detected and classified based on the process acoustics as acoustic emission is considered to be of great potential [13]. This requires correctly annotated acoustic data by various NDT weld inspection methods to later train a classifier. However, annotating the acoustic data manually based on the weld inspection results alone is practically unfeasible because of the acoustic signals not showing indications as clearly as the NDT methods. Defects found during inspection are consequently difficult to locate correctly within the acoustic signal. For the most part, this is due to the acoustic emission by FSW generally not being well understood as there are numerous simultaneous mechanisms that can affect the acoustics. On the contrary side, process data and inspection results are easily understood in comparison. Especially, the machine data provide important information as it contains the welding trajectory bridging spatial and temporal information. Therefore, to transfer

annotation from NDT to FSW and AI, all involved data are put into a common context, while keeping those fields decoupled to avoid any new workload and enabling each expert domain to contribute their results. This removes any necessity of a single expert possessing knowledge across all domains. The main goal is to allow image annotation from NDT to be transferred to acoustic signals by interlocking both modalities geometrically and temporally to machine data.

2. Methods for data generation and data fusion

2.1 Data acquisition

2.1.1 Machine data

The machine control logs the FSW process over time, which was performed by a KUKA KR500 R2830 MT robot equipped with end effector for FSW with a stationary shoulder. Several key process parameters including plunge force, welding force, tool rotation speed, tool orientation and tool center point (TCP). These are recorded by the PCD507, a monitoring solution by KUKA AG, which enables real-time collection and visualization of machine data. In addition, other data such as axis configuration, currents, etc. are monitored as well. From a programming perspective, each machine data sample represents a scalar value, resulting in a one-dimensional time series over the duration of the process. Figure 2 shows selected parameters (left) and the trajectory (right). The samples are collected at a sampling interval of 12 ms.

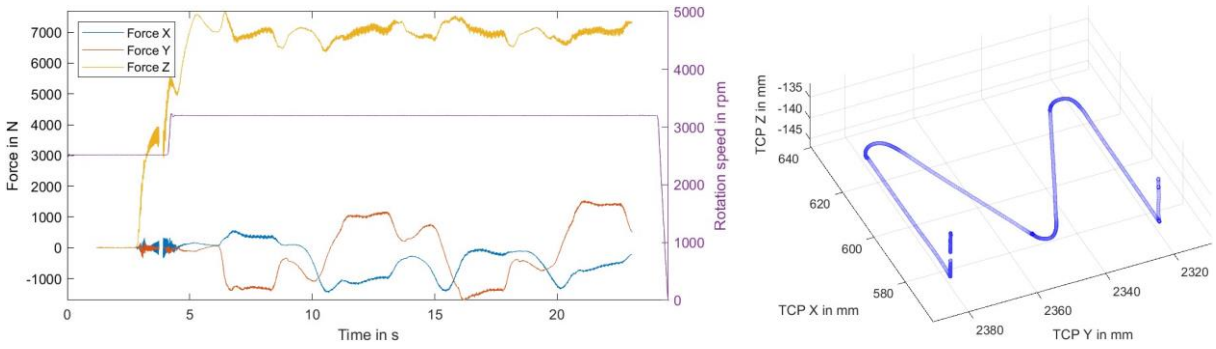

Figure 2. Machine data including forces, spindle speed during the FSW process (left) and trajectory (right)

Figure 2 is described as follows. The tool rotates during the plunging phase with a rotation speed of 2500 rpm. Initially, the tool is not yet in contact with the workpieces and consequently no force is effectively measured. Once the pin moves closer to the workpieces and gets in contact, the force in z-direction rises. At full contact between shoulder and workpieces, a force control system ensures that at a force of 4000 N is asserted. The dwelling phase is skipped. The welding phase starts by tilting the tool at shoulder level by 3 ° (not shown in plot) and continues by increasing the force in z-direction to 7000 N during welding. As the tool moves in the xy-plane in the shape of the letter “M”, resistive forces in x- and y-direction occur accordingly. It may seem contradictory that force in y-direction increases when welding occurs in x-direction. This is simply because the tool itself has its separate coordinate system that was rotated by 90 ° relative to the base coordinate system in which the trajectory is plotted. In the end the tool is retracted, and the force immediately stops measuring as there is supposedly no force during retraction.

2.1.2 Structure borne sound / acoustic emission

Structure borne sound is acquired by acoustic emission sensors, namely Fujicera 1045S, during the FSW process. The sensor is mounted onto the FSW end effector and collects acoustic data at a sample rate of 2.5 MHz, using the PROFile measurement system by BCMtec as shown on

the left of figure 3. An exemplary acoustic emission signal is shown in figure 3 on the right, captured during the welding for seven consecutive overlap joints of two 3 mm thick aluminum (EN AW-6082) plates. While the active FSW process phases are visually apparent by increased amplitudes, it is virtually impossible to determine the exact process transitions through its phases. Furthermore, the tool position at each time is unknown and does not change uniformly as the tool movement typically accelerates and decelerates multiple times during the process. This is indicated in the trajectory of figure 2 by the differing sample density at path positions whenever the path changes orientation. Hence, acoustic signal and machine data need to be first synchronized before further statements can be given on the acoustic signals.

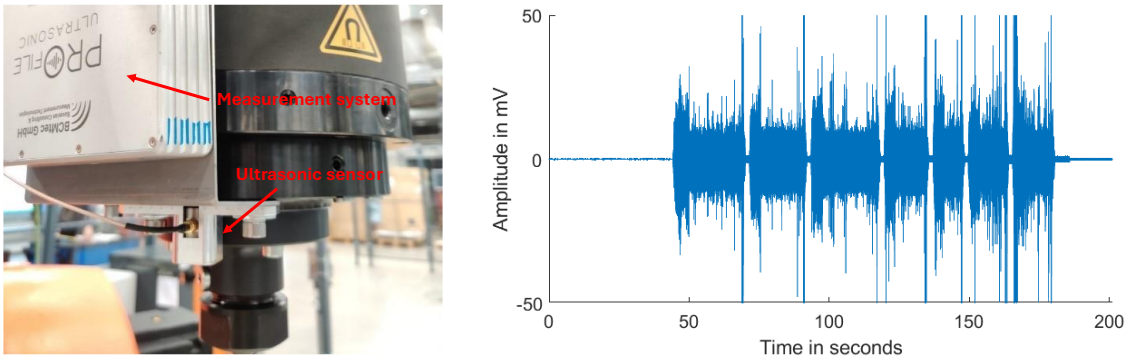

Figure 3. Integration of acoustic emission sensor onto spindle on the left and an example structure borne sound signal during the FSW process shown on the right

2.1.3 Visual inspection

Visual inspection is performed to identify surface irregularities, which can then be annotated as illustrated in figure 4 showing examples of a defect-free weld seam (top) and a weld seam with an annotated surface void (bottom) with EN AW-5754 as material. The off-center defect was caused on purpose by changing rotation speeds from 2800 rpm to 3200 rpm while welding speed was kept constant at 1.5 m/min to initiate abnormal stirring outside the optimal process parameter window. At higher rotation speeds, this flaw becomes even more apparent. The defect was caused by higher shear forces on the advancing side of the joint, where tool rotation and translation move in the same direction as the tool moves from left to right and rotates counterclockwise. In contrast, the retreating side was typically found to be free of such irregularities where tool rotation and translation move in opposite directions, leading to different material flow behavior and comparably lower shear forces than on the advancing side. When considering tool orientation, the material on the advancing side is sheared upward while material on the retreating side is sheared downward, which results in a smoother and more stable flow.

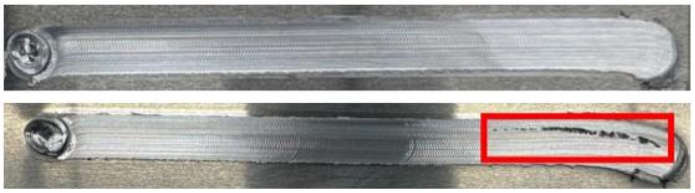

Figure 4. Visual inspection of defect-free overlap weld (top) and overlap weld with surface void (bottom), welding direction from right to left with counterclockwise pin rotation

Such defect is to be rejected according to DIN-ISO 25239-5 [12]. Hence, the surface void is annotated e.g. manually by drawing a bounding box. Such annotations are later correlated to the machine data and the acoustic signals. Alternatively, this step can be automated using segmentation techniques as shown in figure 5, which shows a weld seam that was welded with

a rotation speed of 3500 rpm and measured, using the VHX-7000 digital microscope by Keyence to capture the 3D height profile of the weld seam. Such height profiles can be used for quantitative evaluation of surface grooves, roughness and flashes. These can also be segmented to highlight the surface void to generate an annotation by thresholding the profile to check for significant deviations from the base material height, caused by the surface void.

Figure 5. Segmentation of surface defects based on height profile

2.1.4 Radiography

Radiographic testing is performed using the CT-machine Phoenix Nanotom M to inspect volumetric defects. Shadow scans were taken to find any indications of e.g. lack of materials. Figure 6 shows an example of a weld seam (EN AW-6082) containing a tunnel defect along its welding path in a 2D view. This defect was caused by an increased welding speed of 2.58 m/min at a rotation speed of 3200 rpm, which reduced the material softening and eventually insufficient plastification resulting in void formation. This is also described in [14], though the welding and rotation speed were comparatively low, the highest welding speed being 585 mm/min and rotation speed being 1700 rpm. These radiographic scans are annotated as shown in section 2.3.3.

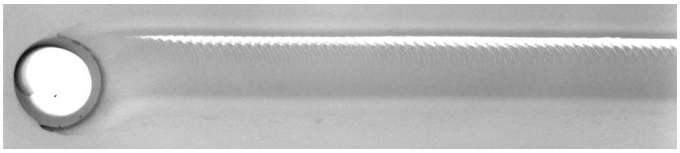

Figure 6. Shadow scan of a weld joint with a tunnel defect along its path

To get a better understanding of the identified indications and to further characterize their location and size in 3D, the weld seams are inspected with computed tomography (CT). For this purpose, a specimen is cut from the whole welded workpiece and put under CT-scanning. The acquired images were then reconstructed in 3D and the defects were segmented, using the software Avizo as shown in figure 7. Technically, these segments can be used as annotations as well, but this approach is not preferred due to the long scanning time. Instead, the CT scan was only utilized to get a better understanding of frequently occurring indications.

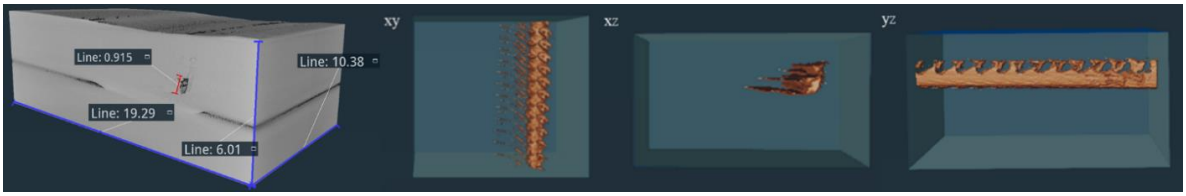

Figure 7. Volume render of 3D reconstructed specimen and segmentation of defects, lengths in mm. Welding direction from front-side to back-side of the specimen.

2.2 Data fusion

Since machine data provides the most direct representation of the process, it is used as the foundational reference for establishing a unified context across all data modalities. Effectively,

there are two problems to be solved: 1) Synchronizing machine data and structure borne sound; 2) Defining a common base coordinate system to align 2D inspection results with machine data. The data fusion is achieved through a multi-step pipeline. First, machine data and acoustic signals are synchronized in time, allowing each acoustic sample to be associated with a tool position. Second, both machine and inspection data are geometrically aligned to have the machine data serve as an information bridge translating spatial information from inspection outputs into temporal information within the acoustic signals, enabling an automatic transfer of inspection annotations directly to the corresponding segments of acoustic data. This is achieved by methods such as perspective correction and image stitching. Temporal synchronization is achieved by cross-correlation of selected machine data and characteristics of acoustic data. Here the rotation speed and the root mean square amplitude of the acoustic signals were correlated based on the physical understanding that acoustic emission occurs as soon as the tool rotates.

2.2.1 Perspective correction

Perspective correction is a method to adjust the perspective or viewpoint of an image to a different position. Here, the purpose of such transformation it to move, stretch and rotate the inspection images, so that it can be put into a coordinate system that also contains the tool center points from machine data and share a common spatial reference. An exemplary perspective correction is visualized in figure 8, where a tilted welded plate is turned front facing and its edges become parallel to the coordinate axis of machine data. This is achieved through a geometric image transformation, which maps control points of an original image to other positions, creating a new image that appears as if it were taken from a different perspective.

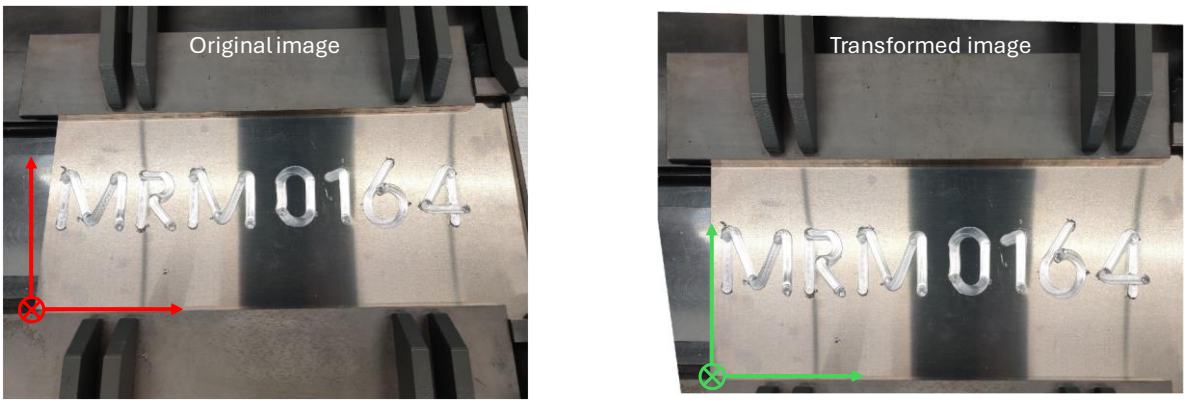

Figure 8. Perspective correction of an original image to align image to machine coordinate system

The perspective correction is implemented as a transformation using a homography matrix H that maps a point (x, y) in the distorted image onto a new position (x', y') by

$$\bar{s}'\begin{bmatrix} x' \\ y' \\ 1 \end{bmatrix} = \begin{bmatrix} \bar{x}' \\ \bar{y}' \\ \bar{s}' \end{bmatrix} = H\begin{bmatrix} x \\ y \\ 1 \end{bmatrix} = \begin{bmatrix} h_{11} & h_{12} & h_{13} \\ h_{21} & h_{22} & h_{23} \\ h_{31} & h_{32} & h_{33} \end{bmatrix}\begin{bmatrix} x \\ y \\ 1 \end{bmatrix}. \quad (1)$$

For this projective transformation the coordinates are normalized, and the z-coordinates of the points are kept constant to operate the transformation only in the x- and y-direction. Consequently, the transformed coordinates are given by

$$x' = \frac{\bar{x}'}{\bar{s}'} = \frac{h_{11}x + h_{12}y + h_{13}}{h_{31}x + h_{32}y + h_{33}}, \quad y' = \frac{\bar{y}'}{\bar{s}'} = \frac{h_{21}x + h_{22}y + h_{23}}{h_{31}x + h_{32}y + h_{33}}. \quad (2)$$

To determine H, four points in the distorted image are selected and their desired locations in the corrected image are defined. Equations (2) can be used to set up a system of equation

$$Ah = \begin{bmatrix} -x_1 & -y_1 & -1 & 0 & 0 & 0 & x_1x'_1 & y_1x'_1 & x'_1 \\ 0 & 0 & 0 & -x_1 & -y_1 & -1 & x_1y'_1 & y_1y'_1 & y'_1 \\ -x_2 & -y_2 & -1 & 0 & 0 & 0 & x_2x'_2 & y_2x'_2 & x'_2 \\ 0 & 0 & 0 & -x_2 & -y_2 & -1 & x_2y'_2 & y_2y'_2 & y'_2 \\ -x_3 & -y_3 & -1 & 0 & 0 & 0 & x_3x'_3 & y_3x'_3 & x'_3 \\ 0 & 0 & 0 & -x_3 & -y_3 & -1 & x_3y'_3 & y_3y'_3 & y'_3 \\ -x_4 & -y_4 & -1 & 0 & 0 & 0 & x_4x'_4 & y_4x'_4 & x'_4 \\ 0 & 0 & 0 & -x_4 & -y_4 & -1 & x_4y'_4 & y_4y'_4 & y'_4 \end{bmatrix} \begin{bmatrix} h_{11} \\ h_{12} \\ h_{13} \\ h_{21} \\ h_{22} \\ h_{23} \\ h_{31} \\ h_{32} \\ h_{33} \end{bmatrix} = 0 \qquad (3)$$

where h is a vectorized representation of the homography matrix H. The solution is obtained numerically, using e.g. Singular Value Decomposition (SVD) of the equation matrix A, with the last column of the computed right singular vector serving as the solution for H which can then be used for the perspective transformation according to equation (1).

2.2.2 Image stitching

For radiographic inspection, multiple overlapping images of the weld seam were taken along the seam. On one hand this was due to spatial constraints by the machine, on other hand the welds seams can be inspected with increased magnification for more detail. To avoid the tedious work of aligning every single image to the base coordinate system, the images are stitched together to form one coherent image based on a 2D cross-correlation as shown in figure 9.

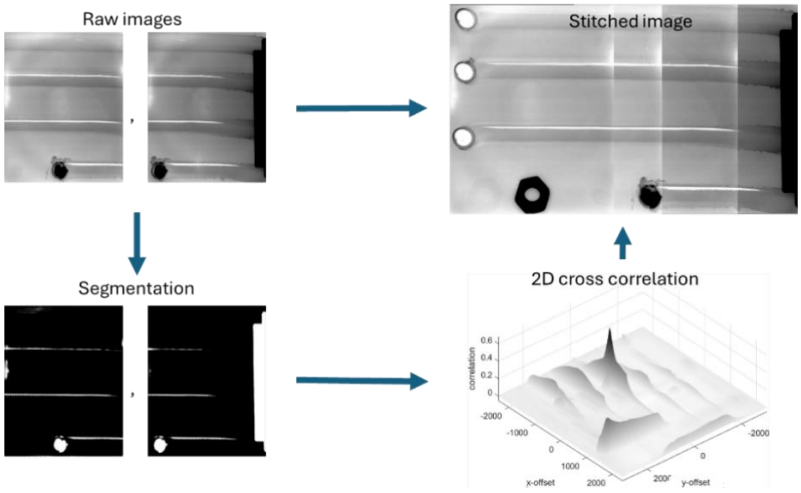

Figure 9. Image processing workflow for image stitching. Radiographic image indications are segmented and cross correlated with the maximum correlation position defining the shift for the stitch.

Raw images are segmented based on a thresholding to highlight indications found in the welding joints. This step also creates a computational advantage as now Boolean matrices instead of raw images are being processed, lowering the computational effort of image processing. The highlighted indications include welding defects, keyholes or other geometries, which were manually introduced during the image acquisition to lower the difficulty of image stitching by additional references. The segmentations are then two-dimensionally cross correlated to find the position of highest similarity between images so that the images can then be shifted relative to each other based on the peak position. In the end this yields the stitched image representing a coherent image of the whole welding joints.

3. Results and discussions

To synchronize the machine data and the acoustic data, the acoustic data was extracted for the root mean square in a sliding window manner with non-overlapping windows of 12 ms, yielding a time series which can be effectively aligned with machine data.

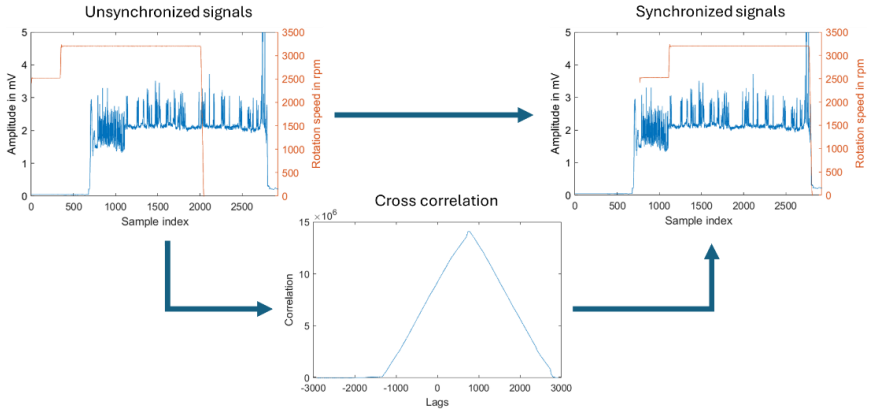

Figure 10. Temporal synchronization of machine data and acoustic signals by cross-correlating tool rotation speed and root mean square amplitude of acoustic signal

The position of the maximum cross correlation was used to align machine data and acoustic data as illustrated in figure 10. Currently, the synchronization accuracy is currently estimated to be within approximately 8 samples or 96 ms. Along a path with welding speed of 1.5 m/min, this corresponds to a spatial precision of 2.4 mm.

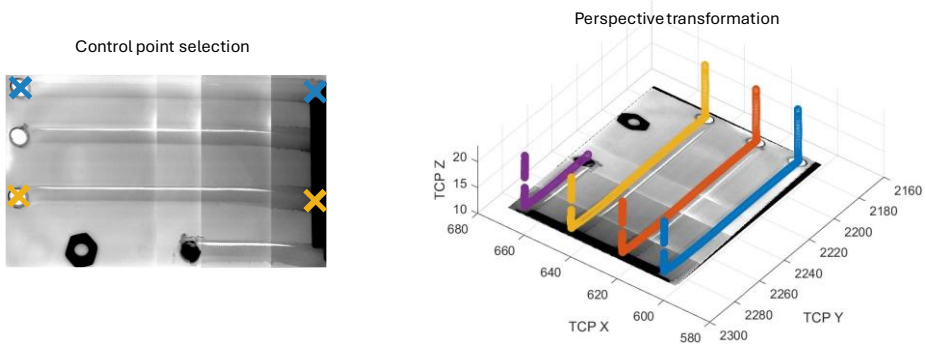

Figure 11. Aligning radiographic images and machine data into a common coordinate system via perspective correction, where control points of the original image were selected at plunge and retraction points

To align the images and machine data to a common coordinate system, perspective correction is used as described in section 2.2.1. Four control points e.g. the position of plunging and retraction points of two weld joints, are selected in the stitched image as indicated in figure 11. The desired control points after transformation are provided by the machine data. The stitched image is then aligned by the homography transformation eq. (1), enabling it to be placed beneath the trajectories without requiring any manual moving, stretching, or rotating the image. Lastly, figure 12 demonstrates the result of the data fusion pipeline and illustrates how annotations from inspection are transferred to the acoustic signal. Seven welding, shaped as the letters “MRM0164” starting at the leftmost letter, joints were generated (refer to section 2.1.2.). When annotations are drawn across the image, these are also shown on the respective time regions within the acoustic signal. This is illustrated for two different regions that are selected as rectangles to provide corresponding annotations.

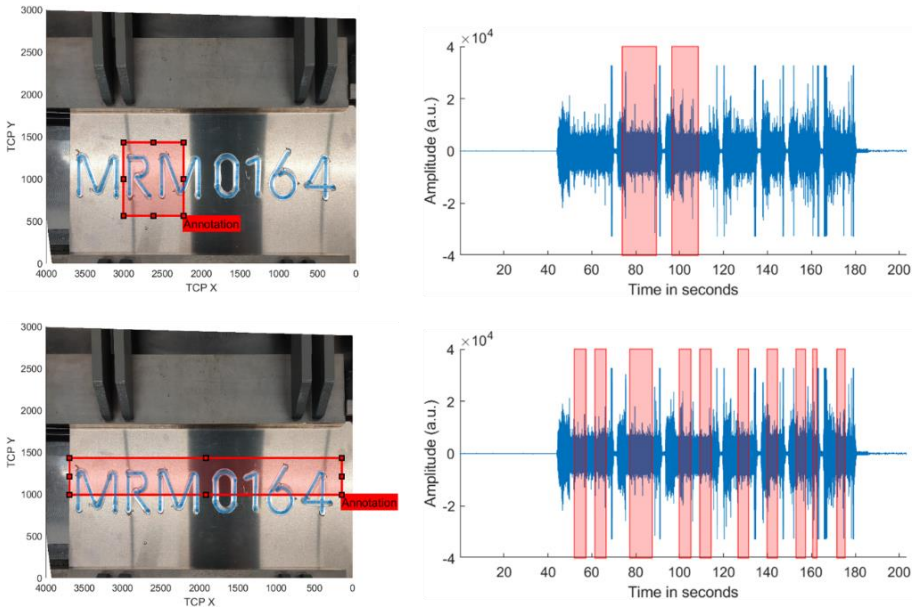

Figure 12. Demonstration of annotation transfer from image to acoustic signal, when image is annotated

The main advantage is that no expert is required who has knowledge across all domains of FSW, NDT and AI to label the information, facilitating more efficient collaborations e.g. allowing a weld inspector to contribute to the generation of an annotated dataset by performing annotations as part of daily work. As positive side effect, efforts in data management and documentation are lowered as all data are curated as a meaningful data set. In principle the shown approach shows potential for any path-based process that shall be monitored online. A similar work focuses on monitoring gas metal arc welding [15], describing how acoustics and video footage of the process can be synchronized to annotate the acoustics through the video annotations, demonstrating the importance of an annotation strategy. On top, this opens a possibility to approach data mining on acoustic data. Most importantly, this enables the training process of supervised learning models for developing an AI-based process monitoring system as correctly annotated data are now available.

Other approaches to make data annotation more efficient focuses on improving collaborations between differing domains. For instance, in reference [16] defining clear instruction for labelling and annotations is recommended. Reference [17] focuses on employing a mix of expert and amateur annotators to lower overall annotation costs. A different work also highlights the importance of such collaborative work in a more general manner, who show that integrating ML into existing systems poses significant challenges due to disciplinary gaps causing issues in communication, documentation, engineering practices, and development processes [18]. Alternatively, effort of data annotation can be reduced by relying less on it. Other methods based on unsupervised, semi-supervised or self-supervised learning can technically remove or at least lower the need for annotations. However, those methods usually come at the cost of worse model performance and furthermore elevate the difficulty of testing and benchmarking as was reviewed for semi-supervised learning methods thoroughly [19].

4. Conclusion

This work exemplary demonstrates how various data modalities acquired during robotic friction stir welding process, from acoustic emissions sensors and from optical NDT inspection methods are combined with machine data to enable transferring specific domain knowledges across involved fields, effectively enabling more effective collaborations among those domain experts

and as result facilitating the generation of annotated data for future applications. A data fusion pipeline was demonstrated, that applies perspective correction to align inspection images weld trajectories within a common coordinate system and synchronizes acoustic data and machine data through cross correlation. This allowed annotations from inspections to be transferred to the acoustic data without manually translating spatial information into its temporal counterpart.

Acknowledgements

The authors like to thank the Free State of Bavaria, represented by the Bavarian State Ministry of Economic Affairs and Media, Energy and Technology, for providing the funding of the project AI for Friction Stir Welding (AI4FSW) within the ZD.B program. We would like to thank VDI/VDE for supervision of the project and the involved industry partners KUKA AG, Grenzebach GmbH, BCMtec GmbH and MT Aerospace AG.

References

1. TAHERI, Hossein; SALIMI BENI, Arefeh. Artificial Intelligence, Machine Learning, and Smart Technologies for Nondestructive Evaluation. Handbook of Nondestructive Evaluation 4.0, 2025
2. VLADOVA, Gergana; HAASE, Jennifer; FRIESIKE, Sascha. Why, with whom, and how to conduct interdisciplinary research? A review from a researcher's perspective. *Science and Public Policy*, 2025, 52. Jg., Nr. 2, S. 165-180.
3. PARK, Soya, et al. Facilitating knowledge sharing from domain experts to data scientists for building nlp models. In: *Proceedings of the 26th International Conference on Intelligent User Interfaces*. 2021.
4. SAMBASIVAN, Nithya, et al. "Everyone wants to do the model work, not the data work": Data Cascades in High-Stakes AI. In: proceedings of the 2021 CHI Conference on Human Factors in Computing Systems. 2021.
5. CUI, Jinhan, et al. Impact of annotation quality on model performance of welding defect detection using deep learning. *Welding in the World*, 2024, 68. Jg., Nr. 4, S. 855-865.
6. MULDOON, James, et al. A typology of artificial intelligence data work. Big data & society, 2024, 11. Jg., Nr. 1, S. 20539517241232632.
7. THOMAS, W. M. Friction stir welding. International Patent Appl. N° PCT/GB92/02203, 1991.
8. MISHRA, Rajiv S.; MA, dan ZY. Friction stir welding and processing. Materials science and engineering: R: reports, 2005, 50. Jg., Nr. 1-2.
9. THREADGILL, P. L., et al. Friction stir welding of aluminium alloys. International Materials Reviews, 2009, 54. Jg., Nr. 2.
10. JAIGANESH, V.; MARUTHU, B.; GOPINATH, E. Optimization of process parameters on friction stir welding of high density polypropylene plate. Procedia Engineering, 2014, 97. Jg., S. 1957-1965.
11. VAIRIS, Achilles, et al. The effect of tool geometry on the strength of FSW aluminum thin sheets. Materials, 2022, 15. Jg., Nr. 22, S. 8187.
12. DIN ISO 25239-5: Friction Stir Welding-Aluminium -Part 5. Deutsches Institut für Normung, 2020.
13. AMBROSIO, Danilo, et al. On the potential applications of acoustic emission in friction stir welding. *Journal of Manufacturing Processes*, 2022, 75. Jg., S. 461-475.
14. ADAMOWSKI, Jarosław; SZKODO, Marek. Friction Stir Welds (FSW) of aluminium alloy AW6082-T6. Journal of Achievements in materials and Manufacturing Engineering, 2007, 20. Jg.
15. MOBARAKI, Mobina, et al. Multi-modal data improves real-time defect classification deep learning models for fillet joints in gas metal arc welding. The International Journal of Advanced Manufacturing Technology, 2025, S. 1-9.
16. LAUX, Johann; STEPHANY, Fabian; LIEFGREEN, Alice. Improving Task Instructions for Data Annotators: How Clear Rules and Higher Pay Increase Performance in Data Annotation in the AI Economy. arXiv preprint arXiv:2312.14565, 2023.
17. LEI, Jiayu, Zhang, Z., Zhang, L., & Li, X. Y. (2022, May). Coca: Cost-effective collaborative annotation system by combining experts and amateurs. In 2022 IEEE 38th International Conference on Data Engineering (ICDE) (pp. 674-685). IEEE.
18. NAHAR, Nadia, et al. Collaboration challenges in building ml-enabled systems: Communication, documentation, engineering, and process. In: Proceedings of the 44th international conference on software engineering. 2022.
19. VAN ENGELEN, Jesper E.; HOOS, Holger H. A survey on semi-supervised learning. Machine learning, 2020, 109. Jg., Nr. 2, S. 373-440.